

ON THE INFLUENCE OF RADIAL COMPONENTS OF  
BLADE FORCES IN AXIAL TURBOMACHINES

Thesis by  
Thorbjorn Karlsson

In Partial Fulfillment of the Requirements  
for the Degree of  
Mechanical Engineer

California Institute of Technology  
Pasadena, California

1953

## ACKNOWLEDGMENT

It gives me great pleasure to acknowledge the interest and assistance offered me by the members of my supervising committee, Mr. Joseph Levy, Dr. H. J. Stewart, and Dr. W. Duncan Rannie. I am particularly indebted to Dr. W. Duncan Rannie, my research advisor, who generously devoted his time to discussions of the problem presented and whose personal encouragement had a strong influence upon my work at the California Institute of Technology.

My grateful thanks are extended to the California Institute of Technology for making my continuation of graduate work possible by the generous grant of a Francis J. Cole Fellowship.

I should also like to express my deep appreciation to my wife, Celeste, who most excellently performed the difficult and tedious task of typing and editing the thesis.

## ABSTRACT

The flow of an incompressible inviscid fluid through a turbomachine with infinite number of blades is investigated in this paper in order to determine the effects of radial forces resulting from the twist of the blades on the flow through the machine.

Prandtl's method of replacing blade rows by distributed vorticity is used and the mathematical problem is treated from that point of view. The flow through the annulus between hub and outer casing of the machine is treated as two-dimensional flow between two parallel flat plates. By assuming a reasonable vorticity distribution throughout the blade row, equations are given which may be applied to calculate the flow induced by radial forces through stationary blade rows. Examples are presented for flow through free vortex and solid body prerotation vanes with radial leading edges. These examples show that the effect of the radial forces resulting from twist is of negligible magnitude.

The effect of leaning the blades in a plane perpendicular to the axis of rotation is investigated. Examples shown indicate that this may be of considerable importance since by leaning the blades it is possible to reduce the axial velocity at the first stage rotor tip and thereby the relative Mach number on the rotor tip.

# TABLE OF CONTENTS

Part	Title	Page
I	Introduction	1
II	Mathematical Formulation of the Problem- Green's Function	5
III	Flow Pattern due to Some Simple Vorticity Distributions	11
	A. Constant Vorticity Concentrated at $x = 0$	11
	B. Constant Vorticity in the Region $-\frac{a}{2} < x < \frac{a}{2}$ , $0 < y < b$	12
	C. Trapezoidal Vorticity Distribution Concentrated at $x = 0$	13
IV	Some Examples of Flow through Stationary Blade Rows	15
	A. Derivation of Equations for Prescribed Blade Loading and Blade Shapes	15
	B. Determination of Constants for a Given Blade Shape	18
	C. Application to Prerotation Vanes	20
V	Effect of Leaning Blades in Plane per- pendicular to the Axis of Rotation	27

### Summary

The present paper is an investigation of the effects of radial forces on the flow through an axial turbomachine resulting from the twist of the blades. The problem is idealized in that the fluid flowing through the machine is assumed inviscid and incompressible, and the number of blades is infinite so that there is no variation in the tangential direction. Furthermore the fluid flow through the annulus between the hub and the outer casing of the machine is treated as two-dimensional flow between two parallel flat plates.

The flow approaching the blade row is assumed to be purely axial, and using Prandtl's method of replacing the blade row by distributed vorticity through the blade row the radial forces are induced by the tangential component of vorticity. The potential function is found for a single vortex located in the region between the two parallel flat plates. This solution is then used to construct a Green's function describing the potential induced by distributed vorticity throughout the region. In order to study the general behavior of the flow a few examples are presented for some very simple cases of distributed vorticity.

The Green's function is used to obtain the general equations for flow through stationary blade rows with prescribed blade loading and prescribed blade shape assuming a reasonable forcing function on the blades. These equations can be used to obtain approximate solutions for flow induced

by any kind of blades. Examples are presented for two types of prerotation vanes with radial leading edges, namely free vortex blades and solid body blades. These examples indicate that the flow field induced by the radial forces is of negligible magnitude. The maximum axial velocity induced for the solid body blades is only about 1.6 per cent of the oncoming axial velocity whereas the maximum radial velocity for the same blades is about 1.2 per cent of the oncoming axial velocity. The deflection of the streamlines is also of very small magnitude. The maximum deflection occurs within the blade row, and for solid body blades this amounts to approximately 0.5 per cent of the spacing between the hub and the outer casing. The free vortex blades show even smaller effect of the radial forces or on the average about one-third of the values obtained for solid body blades. Since it is common practice to construct the blades in such a way that they are radial close to the quarter chord point, the radial forces in front of and behind that point will tend to cancel each other. The effects of the radial forces for this case will therefore be even smaller than the examples treated here indicate.

An investigation is made of the effect of leaning the blades in a plane perpendicular to the axis of rotation. Some examples are presented for various aspect ratio blades and various types of loading. It is found that this method may prove useful to reduce the axial velocity at the tip of the first stage rotor and thereby the relative Mach number

at the rotor tip. Greatest reduction is obtained with blades of high aspect ratio on which the maximum loading is near the trailing edge. By leaning the blades as far as 45 degrees it is found that a reduction in relative velocity as high as 10 per cent for the solid body blade type and about 5 per cent for the free vortex type can be obtained.

## I. INTRODUCTION

For the investigation of flow around finite wings Prandtl (Ref. 1) introduced the simplifying concept of bound and trailing vortex elements. This method has been widely used in problems of flow around single airfoils and may also be used to describe the flow through an axial turbomachine. In the real turbomachine a viscous, compressible fluid flows through an axially symmetric channel. In a region of this channel a system of blades, either stationary or rotating about the axis of symmetry, acts on the fluid. The flow field is thus bounded by the surfaces of the blades as well as by the channel boundaries and is not circumferentially uniform. The total energy of the fluid is nonuniform, the flow is generally rotational, and for rotating blades the flow is unsteady. The real problem is therefore very complicated and cannot be solved exactly by any known methods. Some simplifying assumptions must therefore be made in order to obtain solutions to the problem. One assumption, which always has been made in problems of this type, is that the fluid is nonviscous. This assumption simplifies the problem greatly and gives good results since viscous effects are actually very slight except near the boundaries. Another assumption which is very often made is that the fluid is incompressible. At gas velocities below



the speed of sound compressibility plays a minor role, so that this assumption is good as long as the flow through the machine is subsonic.

A brief review of the earlier important investigations of the flow in turbomachines is given by Marble and Michelson (Ref. 2). These earlier investigations were concerned primarily with the flow through a typical annulus of small radial extent and hence the flow was treated as essentially two-dimensional.

The first detailed analysis of the three dimensional incompressible flow in turbomachines was given by Meyer (Ref. 3) in his consideration of the flow through a stationary blade row. Meyer gives the solution for the blade row in which the flow is irrotational upstream and downstream although the flow within the blade row may be rotational and of a complicated nature. By assuming an infinite number of blades, Meyer treated the problem as tangentially uniform, and then by Fourier analysis these results were modified to obtain the solution for a finite number of blades.

Marble (Ref's 2 and 4) linearized the rotational incompressible flow problem with an infinite number of blades by the assumption that the vorticity is transported along the streamlines of an irrotational flow within the same boundaries. He provided examples of axial flow and conical flow, and stated that the simple linearized solution was sufficiently accurate if the vorticity effects are small.

A second order linearization was also given to handle problems in which the vorticity effects are large.

In the real machine which has a finite number of blades, each blade exerts a force on the fluid. If no viscous forces are present, this blade force must be perpendicular to the blade surface. In general, therefore, this force will have components in the radial and axial directions as well as in the tangential direction. The radial blade force component results from the twist of the blades, and only in blades generated by purely radial lines would this component vanish. In almost all papers on the subject of flow through turbomachines the radial component of the blade forces has been neglected with the exception of Meyer's paper (Ref. 3) in which the radial forces are treated to some extent for free vortex blades.

The present analysis is an investigation of the effects of radial forces on the flow through a turbomachine. The problem is idealized in the sense that the fluid is assumed inviscid and incompressible and the number of blades is infinite. Furthermore the annulus between the hub and the outer casing of the machine is taken as two-dimensional, that is the investigation is made for flow between two parallel flat plates of infinite extent. The assumption that the number of blades is infinite makes the solution of the problem easier in that the flow depends only on two coordinates. The concentrated blade forces are essentially replaced by a body force field distributed throughout the blade region. The two-

dimensional treatment of the problem seems justified, since the analysis becomes greatly simplified, and earlier investigations indicate that solutions obtained by this method ordinarily give good approximations to those obtained by three-dimensional methods.

Prandtl's method of describing the flow through the blade row by replacing the blades by vortex elements thus reduces the problem to finding the flow field due to a continuous vorticity throughout the blade row region. It is assumed that the oncoming flow is purely axial and therefore the radial forces are induced by the tangential component of vorticity. The analysis is made for prescribed radial vorticity component and prescribed blade shape, such that the tangential vorticity component is easily found.

In order to find the flow developed by the tangential component of vorticity, the potential induced by a single vortex between the two flat plates is found. Then a Green's function is constructed such that the flow can be found for arbitrarily distributed vorticity. The general theory is developed in Part II, and some simple examples are presented in Part III. These examples show the general behavior of the flow field. Part IV deals with some examples of flow through free vortex and solid body prerotation vanes with radial leading edges. In Part V is shown an example of the effect of leaning the blades in a plane perpendicular to the axis of rotation of the machine. This study was made in order to determine the possibility of reducing the relative velocity at the first stage rotor tip.

## II. MATHEMATICAL FORMULATION OF THE PROBLEM - GREEN'S FUNCTION

The flow is described (Fig. 1) in a Cartesian coordinate system  $x, y, z$ , by the velocity components  $u, v, w$ , respectively. The  $x$ -coordinate corresponds to the axial coordinate, the  $y$ -coordinate is the radial coordinate, and  $z$  is the tangential coordinate. The corresponding axial, radial, and tangential vorticity components are given by

$$\left. \begin{aligned} \gamma_x &= \frac{\partial w}{\partial y} \\ \gamma_y &= -\frac{\partial w}{\partial x} \\ \gamma_z &= \frac{\partial v}{\partial x} - \frac{\partial u}{\partial y} \end{aligned} \right\} \quad (1)$$

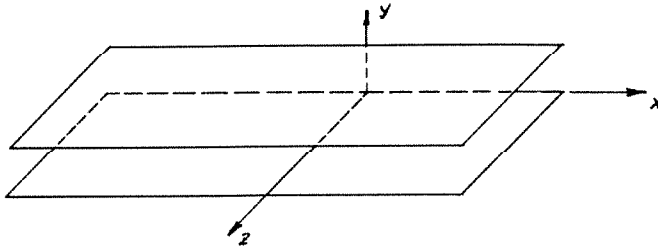


Fig. 1

Because of axial symmetry, only the tangential vorticity is associated with the radial and axial velocities while the radial and axial components of vorticity are associated with the tangential or whirl velocity only. The problem of finding the effect of the radial forces can therefore be treated in the  $(x,y)$ -plane, and the object is to find the potential  $\phi$  due to a single vortex of strength  $\Gamma$  in the region as shown in Figure 2.

The potential satisfies Laplace's equation

$$\frac{\partial^2 \phi}{\partial x^2} + \frac{\partial^2 \phi}{\partial y^2} = 0 \quad (2)$$

$$\left. \begin{aligned} v &= \frac{\partial \phi}{\partial y} = 0 \quad \text{at } y=0 \text{ and } y=b, \text{ all } x \\ \phi &\rightarrow 0 \quad \text{as } x \rightarrow \infty \\ \phi &= 0 \quad \text{for } y < \eta, \quad \phi = -\frac{\Gamma}{2} \text{ for } y > \eta \quad \text{at } x=0 \end{aligned} \right\} \quad (3)$$
$$\frac{x''}{x} + \frac{y''}{y} = 0$$

or 
$$\frac{\chi''}{\chi} = -\frac{Y''}{Y} = \lambda^2 \quad (4)$$

$$\left. \begin{aligned} X &= e^{\pm i y} \\ Y &= \begin{cases} \cos y \\ \sin y \end{cases} \end{aligned} \right\} \quad (5)$$

From boundary conditions at  $x = \infty$ , it is clear that the potential must be on the form

$$\phi = (A \cos \lambda y + B \sin \lambda y) e^{-\lambda x} \quad (6)$$

Taking the derivative of this with respect to  $y$  gives

$$\frac{\partial \phi}{\partial y} = \lambda (-A \sin \lambda y + B \cos \lambda y) e^{-\lambda x}$$

Therefore from boundary conditions at  $y = 0$  and  $y = b$  this gives

$$B = 0$$

$$\lambda = \frac{n\pi}{b} \quad n = 1, 2, 3, \dots \quad (7)$$

The case  $\lambda = 0$  gives a different form of solution. For that case (4) becomes

$$\left. \begin{aligned} X'' &= 0 \\ Y'' &= 0 \end{aligned} \right\} \quad (8)$$

which has the solutions

$$\left. \begin{aligned} X &= Cx + D \\ Y &= Ey + F \end{aligned} \right\} \quad (9)$$

The solutions given by (9), however, need not be considered here since they cannot satisfy the boundary conditions (3). The particular solution to (2) is therefore on

the form

$$\phi = A_n \cos \frac{n\pi y}{b} e^{-\frac{n\pi x}{b}} \quad n=1,2,3,\dots$$

and since the equation is linear these may be summed over all values of  $n$ . The potential is then

$$\phi = \sum_{n=1}^{\infty} A_n \cos \frac{n\pi y}{b} e^{-\frac{n\pi x}{b}} \quad (10)$$

Now the value of the constants  $A_n$  may be determined since  $\phi$  is known at  $x = 0$ . Putting  $x = 0$  and multiplying both sides of (10) by  $\cos \frac{m\pi y}{b}$  one integrates with respect to  $y$  from  $y = 0$  to  $y = b$ . This gives

$$\int_0^b 0 \cdot \cos \frac{m\pi y}{b} dy - \frac{\Gamma}{2} \int_0^b \cos \frac{m\pi y}{b} dy = \sum_{n=1}^{\infty} A_n \int_0^b \cos \frac{m\pi y}{b} \cos \frac{n\pi y}{b} dy$$

or

$$\frac{\Gamma}{2} \cdot \frac{b}{\pi n} \sin \frac{n\pi \eta}{b} = A_n \frac{b}{2}$$

i.e.

$$A_n = \frac{\Gamma}{\pi} \cdot \frac{\sin \frac{n\pi \eta}{b}}{n} \quad (11)$$

For the region  $x < 0$  the following boundary conditions apply

$$\left. \begin{aligned} v = \frac{\partial \phi}{\partial y} &= 0 \quad \text{at } y=0 \text{ and } y=b, \text{ all } x \\ \phi &\rightarrow 0 \quad \text{as } x \rightarrow -\infty \\ \phi &= 0 \text{ for } y < \eta, \quad \phi = \frac{\Gamma}{2} \text{ for } y > \eta \text{ at } x=0 \end{aligned} \right\} \quad (12)$$

By the same procedure as before it is found that the potential is given by

$$\phi = \sum_{n=1}^{\infty} A'_n \cos \frac{n\pi y}{b} e^{\frac{n\pi x}{b}} \quad (13)$$

where

$$A'_n = -\frac{\Gamma}{\pi} \cdot \frac{\sin \frac{n\pi \eta}{b}}{n} \quad (14)$$

The potential due to a single vortex of strength  $\Gamma$  located at  $(x,y) = (0,\eta)$  is therefore given by

$$\left. \begin{aligned} \phi &= \frac{\Gamma}{\pi} \sum_{n=1}^{\infty} \frac{\sin \frac{n\pi \eta}{b} \cos \frac{n\pi y}{b}}{n} e^{-\frac{n\pi x}{b}} & x > 0 \\ \phi &= -\frac{\Gamma}{\pi} \sum_{n=1}^{\infty} \frac{\sin \frac{n\pi \eta}{b} \cos \frac{n\pi y}{b}}{n} e^{\frac{n\pi x}{b}} & x < 0 \end{aligned} \right\} \quad (15)$$

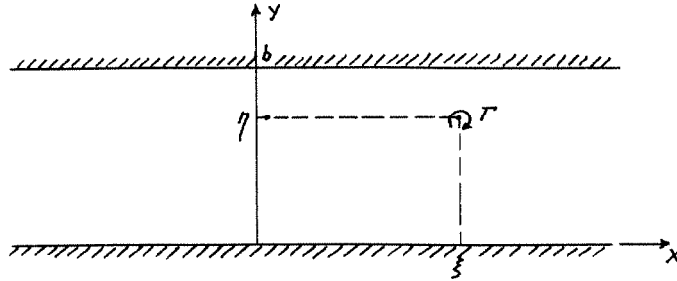


Fig. 3

If the vortex is located at  $(x,y) = (\xi, \eta)$  (Fig. 3) equation (15) becomes

$$\left. \begin{aligned} \phi &= \frac{\Gamma}{\pi} \sum_{n=1}^{\infty} \frac{\sin \frac{n\pi \eta}{b} \cos \frac{n\pi y}{b}}{n} e^{-\frac{n\pi(x-\xi)}{b}} & x > \xi \\ \phi &= -\frac{\Gamma}{\pi} \sum_{n=1}^{\infty} \frac{\sin \frac{n\pi \eta}{b} \cos \frac{n\pi y}{b}}{n} e^{\frac{n\pi(x-\xi)}{b}} & x < \xi \end{aligned} \right\} \quad (16)$$



The Green's function can now easily be constructed. For distributed vorticity  $\gamma(x,y)$  one can replace  $\Gamma$  by  $\gamma(x,y)dxdy$  in equation (16) and integrate over the entire domain. The potential is then

$$\phi = \frac{1}{\pi} \sum_{n=1}^{\infty} \frac{\cos \frac{n\pi y}{b}}{n} \left\{ \int_0^b \int_{-\infty}^x \gamma(\xi, \eta) e^{-\frac{n\pi(x-\xi)}{b}} d\xi - \int_x^{\infty} \gamma(\xi, \eta) e^{\frac{n\pi(x-\xi)}{b}} d\xi \right\} \sin \frac{n\pi \eta}{b} d\eta \quad (17)$$

If the vorticity is concentrated at  $x = 0$  and its distribution is given by  $\gamma = \gamma(y)$  the potential is

$$\left. \begin{aligned} \phi &= \frac{1}{\pi} \sum_{n=1}^{\infty} \frac{\cos \frac{n\pi y}{b}}{n} e^{-\frac{n\pi x}{b}} \int_0^b \gamma(\eta) \sin \frac{n\pi \eta}{b} d\eta & x > 0 \\ \phi &= -\frac{1}{\pi} \sum_{n=1}^{\infty} \frac{\cos \frac{n\pi y}{b}}{n} e^{\frac{n\pi x}{b}} \int_0^b \gamma(\eta) \sin \frac{n\pi \eta}{b} d\eta & x < 0 \end{aligned} \right\} \quad (18)$$

### III. FLOW PATTERN DUE TO SOME SIMPLE VORTICITY DISTRIBUTIONS.

In order to investigate the general behavior of the flow pattern due to distributed vorticity some preliminary calculations were made for some simple distributions, namely constant vorticity concentrated at  $x = 0$ , constant vorticity in the region  $0 < y < b$ ,  $-\frac{a}{2} < x < \frac{a}{2}$ , and trapezoidal vorticity distribution concentrated at  $x = 0$ .

#### A. Constant Vorticity Concentrated at $x = 0$ .

Equation (18) applies for this case. One gets

$$\begin{aligned} \int_0^b \gamma(\eta) \sin \frac{n\pi\eta}{b} d\eta &= \frac{2b\gamma}{n\pi} && \text{for } n \text{ odd} \\ &= 0 && \text{for } n \text{ even} \end{aligned}$$

The potential is therefore

$$\left. \begin{aligned} \phi &= \frac{2b\gamma}{\pi^2} \sum_{n=0}^{\infty} \frac{\cos \frac{(2n+1)\pi y}{b}}{(2n+1)^2} e^{-\frac{(2n+1)\pi x}{b}} && x > 0 \\ \phi &= -\frac{2b\gamma}{\pi^2} \sum_{n=0}^{\infty} \frac{\cos \frac{(2n+1)\pi y}{b}}{(2n+1)^2} e^{\frac{(2n+1)\pi x}{b}} && x < 0 \end{aligned} \right\} \quad (19)$$

The velocity distribution due to this vorticity distribution is shown in Figures 12 and 13. It is to be noted that the axial velocity induced by the vorticity has a

singularity at  $(x,y) = (0,0)$  or  $(x,y) = (0,b)$ . This is, of course, due to the fact that a vortex line cannot have a component parallel to a wall right at the wall. This condition is obviously violated here and the result is that the velocity perpendicular to the wall does not vanish at the wall, which violates the boundary conditions of the problem. This singularity in axial velocity at the wall does not arise if the vorticity is distributed over a finite region in the  $x$ -direction even though the boundary conditions at the wall are not satisfied for this case either. In all physical problems, of course, the vorticity must be distributed over a finite region.

B. Constant Vorticity in the Region  $-\frac{a}{2} < x < \frac{a}{2}$ ,  $0 < y < b$

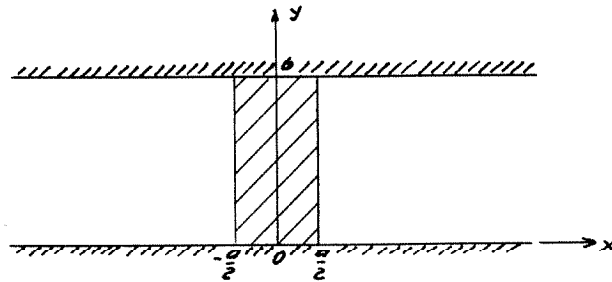


Fig. 4

It was found from the example of a concentrated vorticity at  $x = 0$  that the axial velocity had a singularity at  $(x,y) = (0,0)$ . For the present case it was therefore considered sufficient to calculate the effect of the width  $a$  upon the axial velocity at  $(x,y) = (\frac{a}{2}, 0)$ . The axial velocity

at that point is found to be given by

$$u\left(\frac{a}{2}, 0\right) = -\frac{2rb}{\pi^2} \sum_{n=0}^{\infty} \frac{1}{(2n+1)^2} \left(1 - e^{-\frac{(2n+1)\pi a}{b}}\right) \quad (20)$$

In Figure 14 the values of this maximum axial velocity are plotted as a function of the width of the vorticity region  $a$ . The values of  $u$  were computed for constant total vorticity  $\gamma ab$  so as to make them more easily comparable with the results obtained for case A.

C. Trapezoidal Vorticity Distribution Concentrated at  $x = 0$

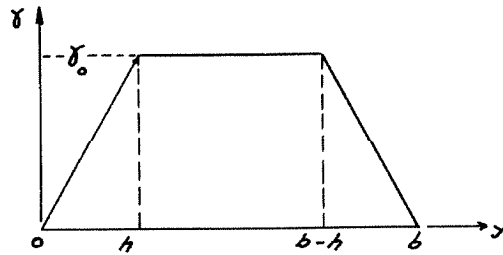


Fig. 5

As was pointed out before it is necessary that the tangential component of vorticity vanish at the boundary. The axial velocity at the point  $(x,y) = (0,0)$  was therefore computed for the vorticity distribution at  $x = 0$  given by Figure 5, i.e.

$$\left. \begin{aligned} \gamma &= \gamma_0 \frac{y}{h} & 0 \leq y \leq h \\ \gamma &= \gamma_0 & h \leq y \leq b-h \\ \gamma &= \gamma_0 \frac{b-y}{h} & b-h \leq y \leq b \end{aligned} \right\} \quad (21)$$

At the point  $(x,y) = (0,0)$  the axial velocity is determined by the series

$$u = - \frac{2\pi b}{h\pi^2} \sum_{n=0}^{\infty} \frac{\sin \frac{(2n+1)\pi h}{b}}{(2n+1)^2} \quad (22)$$

Figure 15 shows the relationship between this maximum axial velocity and the value of  $h$ .

These three simple examples show the general trend of the flow pattern and give an idea about the magnitude of the induced velocity field which can be expected from the various blade forms. Figure 14 shows that a high aspect ratio blade will have a stronger effect on the flow than will a low aspect ratio blade. From Figure 15 it is seen that the induced axial velocity at the hub or the tip is a rather strong function of the layer height,  $h$ , near the walls. This height may be taken as approximately the thickness of the boundary layer.

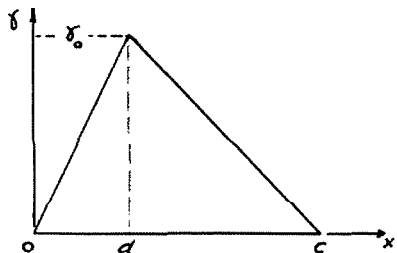
#### IV. SOME EXAMPLES OF FLOWS THROUGH STATIONARY BLADE ROWS

##### A. Derivation of Equations for Prescribed Blade Loading and Blade Shapes

In the following example the flow field induced by a single stationary blade row is determined. Consider a blade row whose blade chord has the axial projection  $c$ , constant for all radii, and prescribe the radial vorticity distribution by

$$\gamma_y = \gamma(x)(1 + \beta y) \quad (23)$$

where  $\gamma(x)$  (see Fig. 6) is given by



$$\left. \begin{aligned} \gamma(x) &= 0 & x &\leq 0 \\ \gamma(x) &= \gamma_0 \frac{x}{a} & 0 \leq x \leq a \\ \gamma(x) &= \gamma_0 \frac{c-x}{c-a} & a \leq x \leq c \\ \gamma(x) &= 0 & c \leq x \end{aligned} \right\} \quad (24)$$

Fig. 6

The tangential component of the vorticity is obtained by multiplying the radial component by the tangent of the angle  $\alpha$ , which the blade surface makes with a radial line through each point of the blade surface. Assume that the tangent is a linear function of  $x$  only, i.e.

$$\tan \alpha = l + mx \quad (25)$$

The tangential component of vorticity is therefore given by

$$\delta_z = \delta(x)(1+\beta y)(1+mx) \quad (26)$$

However, as was pointed out previously, it is necessary that the tangential component of vorticity vanish at the walls, and therefore equation (26) is multiplied by the function  $f(y)$  shown in Figure 7, i.e.

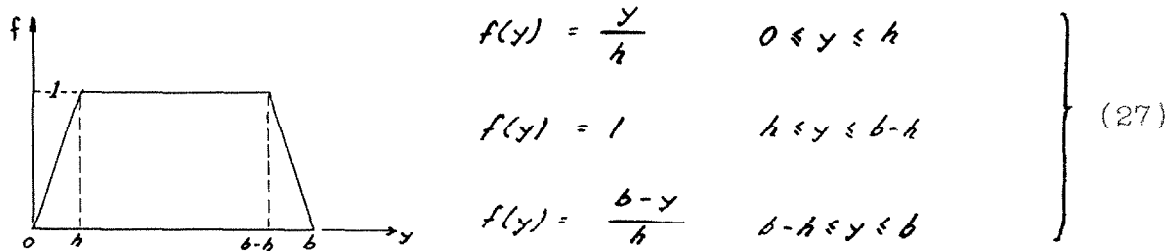


Fig. 7

Tangential vorticity then becomes

$$\delta_z = \delta(x)(1+\beta y)(1+mx)f(y) \quad (28)$$

Equation (17) can now be applied and the potential found for the four regions  $x \leq 0$ ,  $0 \leq x \leq d$ ,  $d \leq x \leq c$ , and  $c \leq x$ . After rather lengthy algebra the equations shown on the next page are obtained, and these can now be applied in order to determine the flow field for the various kinds of blading.

VELOCITY POTENTIAL DUE TO VORTICITY GIVEN BY EQ. (28)

REGION 1:  $-\infty < x \leq 0$

$$\phi = \frac{\gamma_0 b^4}{h d (c-d) \pi^5} \sum_{n=1}^{\infty} \frac{\cos \frac{n\pi y}{b}}{n^5} e^{\frac{n\pi x}{b}} A_n \left\{ \left( c \left( 1 - e^{-\frac{n\pi d}{b}} \right) - d \left( 1 - e^{-\frac{n\pi c}{b}} \right) \right) - m c d \left( e^{\frac{n\pi c}{b}} - e^{\frac{n\pi d}{b}} \right) - \frac{2bm}{n\pi} \left( d \left( 1 - e^{-\frac{n\pi c}{b}} \right) - c \left( 1 - e^{-\frac{n\pi d}{b}} \right) \right) \right\}$$

REGION 2:  $0 \leq x \leq d$

$$\phi = \frac{\gamma_0 b^4}{h d (c-d) \pi^5} \sum_{n=1}^{\infty} \frac{\cos \frac{n\pi y}{b}}{n^5} A_n \left\{ \left( c-d \right) e^{\frac{n\pi x}{b}} - 2 \left( 1 + 2mx \right) \left( c-d \right) + c \left( 1 + md \right) e^{\frac{n\pi (c-x)}{b}} - d \left( 1 + mc \right) e^{\frac{n\pi (d-x)}{b}} + \frac{2bm}{n\pi} \left( c \left( e^{\frac{n\pi (c-x)}{b}} - e^{\frac{n\pi (d-x)}{b}} \right) - d \left( e^{\frac{n\pi (c-x)}{b}} - e^{\frac{n\pi (d-x)}{b}} \right) \right) \right\}$$

REGION 3:  $d \leq x \leq c$

$$\phi = \frac{\gamma_0 b^4}{h d (c-d) \pi^5} \sum_{n=1}^{\infty} \frac{\cos \frac{n\pi y}{b}}{n^5} A_n \left\{ \left( c-d \right) e^{\frac{n\pi x}{b}} + 2 d \left( 1 + m \left( 2x - c \right) \right) - c \left( 1 + md \right) e^{\frac{n\pi (x-d)}{b}} - d \left( 1 + mc \right) e^{\frac{n\pi (x-d)}{b}} + \frac{2bm}{n\pi} \left( c \left( e^{\frac{n\pi (x-d)}{b}} - e^{\frac{n\pi (c-x)}{b}} \right) - d \left( e^{\frac{n\pi (x-d)}{b}} - e^{\frac{n\pi (c-x)}{b}} \right) \right) \right\}$$

REGION 4:  $c \leq x < \infty$

$$\phi = \frac{\gamma_0 b^4}{h d (c-d) \pi^5} \sum_{n=1}^{\infty} \frac{\cos \frac{n\pi y}{b}}{n^5} e^{\frac{n\pi x}{b}} A_n \left\{ \left( c \left( 1 - e^{-\frac{n\pi d}{b}} \right) - d \left( 1 - e^{-\frac{n\pi c}{b}} \right) \right) + m c d \left( e^{\frac{n\pi c}{b}} - e^{\frac{n\pi d}{b}} \right) + \frac{2bm}{n\pi} \left( d \left( 1 - e^{-\frac{n\pi c}{b}} \right) - c \left( 1 - e^{-\frac{n\pi d}{b}} \right) \right) \right\}$$

where

$$A_n = \left[ 1 - (-1)^n + (1 + (-1)^n) \rho h - (-1)^n \rho b \right] \sin \frac{n\pi h}{b} - \frac{2 \rho b}{n\pi} (1 + (-1)^n) \left( 1 - \cos \frac{n\pi h}{b} \right)$$



### B. Determination of Constants for a Given Blade Shape

The constants  $\gamma_0$ ,  $\beta$ ,  $l$ , and  $m$  have to be determined for each given blade shape. Assuming that the whirl velocity approaching the blade row is zero, the whirl velocity downstream is given by

$$c_u = \int_0^c \gamma_y dx \quad (29)$$

Now the prescribed radial vorticity distribution is given by equation (23) and equation (29) gives therefore

$$c_u = \frac{\gamma_0 c}{2} (1 + \beta y) \quad (30)$$

This gives a linear distribution of whirl velocity which obviously does not satisfy all given blade shapes. The constants  $\gamma_0$  and  $\beta$  will therefore be chosen so as to fit the given whirl velocity distribution as near as can be done by a straight line.

The constants  $l$  and  $m$  still remain to be determined. The tangent of the angle which the blade makes with a radial line was given by equation (25)

$$\tan \alpha = l + mx$$

Therefore if the blade surface is given by  $z = z(x, y)$  this gives

$$\frac{\partial z}{\partial y} = l + mx \quad (31)$$

If the blade is given such that it is radial at a certain axial position,  $x = x_0$ , then

$$\left. \frac{\partial z}{\partial y} \right|_{x=x_0} = l + mx_0 = 0$$

or

$$l = -mx_0 \quad (32)$$

Therefore

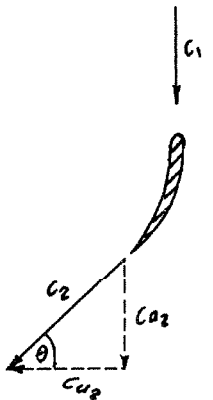
$$\frac{\partial z}{\partial y} = m(x - x_0) \quad (33)$$

Integrating this gives

$$z = m(x - x_0)y + f(x) \quad (34)$$

where  $f(x)$  is an arbitrary function of  $x$ .

Now for a given blade shape the trailing edge angle,  $\theta$ , is known. Assuming that the flow leaves the trailing edge tangential to the trailing edge (Fig. 8) equation (34) gives



$$\left. \frac{\partial z}{\partial x} \right|_{x=c} = my + f'(c)$$

$$= \cot \theta(y)$$

$$= \frac{c_{u2}}{c_{a2}}$$

}

(35)

fig. 8

Again this is an approximation to the real blade and the

constant  $m$  will be determined so as to satisfy equation (35) approximately.

### C. Application to Free Vortex and Solid Body Prerotation Vanes.

This is now applied to free vortex and solid body prerotation vanes with radial leading edges. It is assumed that the flow upstream is purely axial with a constant velocity  $c_a$ . The following data are used

$$\frac{c}{b} = 0.25$$

$$\frac{h}{b} = 0.1$$

$$\frac{d}{c} = 0.25$$

Hub ratio = 0.6

$$\frac{c_a}{U} = 0.45$$

where  $U$  = tip velocity of rotating blades

For free vortex blades

$$\frac{c_u}{U} = \frac{0.145}{\xi}$$

For solid body blades

$$\frac{c_u}{U} = 0.325 \xi$$

where  $\xi = \frac{r}{r_0} = 0.6 + 0.4 \frac{y}{b}$  is a dimensionless radius

$r_0$  = tip radius

The choice of  $c$ ,  $d$ , and  $h$  made here is arbitrary, but the value chosen for  $h$  is of the same order of magnitude as the boundary layer thickness. The other data are taken from the axial flow compressor described in Reference 5.

## 1. Free vortex blades

The whirl velocity is given by

$$\frac{c_u}{U} = \frac{0.145}{\xi} = \frac{0.725}{3 + 2\frac{y}{b}}$$

Equation (30) gives therefore

$$\frac{r_o c}{2U} (1 + \beta y) \approx \frac{0.725}{3 + 2\frac{y}{b}} \quad (36)$$

For this case the axial velocity is unchanged going through the blade row so that equation (35) gives

$$\cot \theta(y) = \frac{c_u}{c_a} = \frac{0.725}{0.45(3 + 2\frac{y}{b})}$$

or

$$f'(c) + my \approx \frac{0.725}{0.45(3 + 2\frac{y}{b})} \quad (37)$$

From Figure 16, this gives the following approximate values

$$\begin{aligned} \frac{r_o c}{2U} &= 0.235 \\ \beta &= -\frac{0.409}{b} \\ m &= -\frac{0.215}{b} \end{aligned}$$

## 2. Solid body blading

For the solid body blading the whirl velocity is

$$\frac{c_u}{U} = 0.325\xi = 0.195 + 0.13\frac{y}{b}$$

Equation (30) gives then

$$\frac{r_0 c}{2U} (1 + \beta y) = 0.195 + 0.13 \frac{y}{b} \quad (38)$$

This gives

$$\frac{r_0 c}{2U} = 0.195$$

$$\beta = \frac{0.667}{b}$$

The determination of the constant  $m$  is not so simple in the case of solid body blades as it is for the free vortex blades, since here the axial velocity downstream from the blades is not constant. In order to determine the axial velocity downstream the following equations apply

Bernoulli equation

$$\frac{p_1}{\rho} + \frac{1}{2}(c_{u1}^2 + c_{a1}^2) = \frac{p_2}{\rho} + \frac{1}{2}(c_{u2}^2 + c_{a2}^2) \quad (39)$$

Radial equilibrium

$$\left. \begin{aligned} \frac{dp_1}{dr_1} &= \rho \frac{c_{u1}^2}{r_1} \\ \frac{dp_2}{dr_2} &= \rho \frac{c_{u2}^2}{r_2} \end{aligned} \right\} \quad (40)$$

Continuity equation

$$r_1 c_{a1} dr_1 = r_2 c_{a2} dr_2 \quad (41)$$

Subscript 1 refers to conditions upstream and subscript 2 refers to conditions downstream from the blade row.

Differentiation of equation (39) gives

$$\left[ \frac{1}{\rho} \frac{d\rho}{dr_1} + \frac{1}{2} \frac{d}{dr_1} (c_{u_1}^2 + c_{a_1}^2) \right] dr_1 = \left[ \frac{1}{\rho} \frac{d\rho}{dr_2} + \frac{1}{2} \frac{d}{dr_2} (c_{u_2}^2 + c_{a_2}^2) \right] dr_2 \quad (42)$$

which may be written making use of equations (40) and (41)

$$\frac{1}{r_2 c_{a_2}} \left[ \frac{1}{r_2^2} \frac{d}{dr_2} (r_2^2 c_{u_2}^2) + \frac{d}{dr_2} (c_{a_2}^2) \right] = \frac{1}{r_1 c_{a_1}} \left[ \frac{1}{r_1^2} \frac{d}{dr_1} (r_1^2 c_{u_1}^2) + \frac{d}{dr_1} (c_{a_1}^2) \right] \quad (43)$$

For the solid body blading the right hand side of equation (43) vanishes since

$$\begin{aligned} c_{u_1} &= 0 \\ c_{a_1} &= \text{constant} \end{aligned}$$

Also

$$c_{u_2} = \alpha_2 \xi = \alpha_2 \frac{r}{r_0} \quad \text{with} \quad \alpha_2 = 0.325$$

Equation (43) is then reduced to

$$\begin{aligned} \frac{\alpha_2^2}{r_0^2 r^2} \frac{d(r^4)}{dr} + \frac{d(c_{a_2}^2)}{dr} &= 0 \\ \text{or} \quad \frac{d(c_{a_2}^2)}{dr} &= -4 \frac{\alpha_2^2}{r_0^2} r \end{aligned} \quad (44)$$

Integration of this gives

$$c_{a_2} = \alpha_2 \sqrt{2} \sqrt{A - \left(\frac{r}{r_0}\right)^2} = \alpha_2 \sqrt{2} \sqrt{A - \xi^2} \quad (45)$$

The constant A is found from the continuity equation

$$\int_{r_1}^{r_0} c_{a_1} r_1 dr_1 = \int_{r_1}^{r_0} c_{a_2} r_2 dr_2 \quad (46)$$

This gives

$$\frac{C_{a2}}{U} = 0.325 \sqrt{2} \sqrt{1.625 - \xi^2} \quad (47)$$

Therefore

$$\cot \theta(y) = \frac{C_{u2}}{C_{a2}} = \frac{\xi}{\sqrt{3.25 - 2\xi^2}} \quad (48)$$

Equation (35) gives

$$f'(c) + my \approx \frac{\xi}{\sqrt{3.25 - \xi^2}} \quad (49)$$

Figure 17 gives then the approximate value for m

$$m = \frac{0.477}{b}$$

The results for free vortex and solid body blades are shown in Table I below

Table I

Values of the constants  $\gamma_0$ ,  $\beta$ , and  $m$  for free vortex and solid body prerotation vanes with radial leading edges

	Free Vortex	Solid Body
$\frac{\gamma_0 c}{2U}$	0.235	0.195
$\beta b$	-0.409	0.667
$mb$	-0.215	0.477

Using these constants calculations were made of the velocity field behind the blade row at two stations, namely at the trailing edge and at one chordlength away from the trailing edge. The results are presented in Figures 18 and 19. Also the radial velocity distribution at midradius and the deflection of the streamlines were calculated through the blade row. These are shown in Figures 20 and 21 respectively. All these results show that the velocity field induced by prerotation vanes with radial leading edges have no appreciable effect on the flow field through the blade row. The maximum radial velocity is only about 1.2 per cent of the approaching axial velocity for the solid body vanes and less than one third of that for the free vortex blading. The same is true for the induced axial velocity where the maximum is approximately 1.6 per cent of the approaching axial velocity for the solid body and about one third of that for the free vortex blading. The streamlines are deflected a very small amount or only about 0.5 per cent of the spacing between the hub and the outer casing in the case of solid body blading and still less for free vortex vanes.

In case the radial line does not fall on the leading edge of the blade but rather on some other axial position of the blade, the effect of the radial forces will be of even smaller magnitude. Since it is common practice to construct the blades in such a way that they are radial close to the quarter chord point, the radial forces in front of and behind that point will tend to cancel each other. The effects of the



radial forces for this case will therefore be even smaller than the examples treated here indicate.

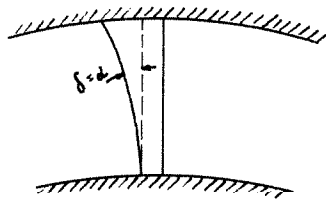
# V. EFFECT OF LEANING THE BLADES IN A PLANE PERPENDICULAR TO THE AXIS

In equation (25) the blade shape was given by

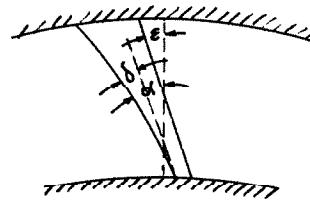
$$\tan \alpha = l + mx$$

where  $\alpha$  is the angle which the blade surface makes with a radial line (see Figure 9). For a radial leading edge this becomes

$$\tan \alpha = mx = \tan \delta$$



a. Untilted Blade



b. Tilted Blade

Fig. 9

Now if the blade is tilted at an angle  $\epsilon$  (Fig. 9,b) this becomes

$$\tan \alpha = \tan(\delta + \epsilon) = \frac{\tan \delta + \tan \epsilon}{1 - \tan \delta \tan \epsilon}$$

It was found previously that  $\tan \delta = mx$  is a very small quantity so that this may be written approximately

$$\tan \alpha \approx \tan \delta + \tan \epsilon = l + mx \quad (50)$$

i.e.

$$\tan \epsilon = l \quad (51)$$

The tilting of the blades may be used to an advantage in order to decrease the axial velocity at the tip and thus reduce the relative Mach number at the rotor tip. If this reduction is found to be appreciable this is of great importance in compressor design since the Mach number at the first stage rotor tip is one of the limiting factors in compressor design. The velocity diagram shown in Figure 10 shows how this reduction may be accomplished.

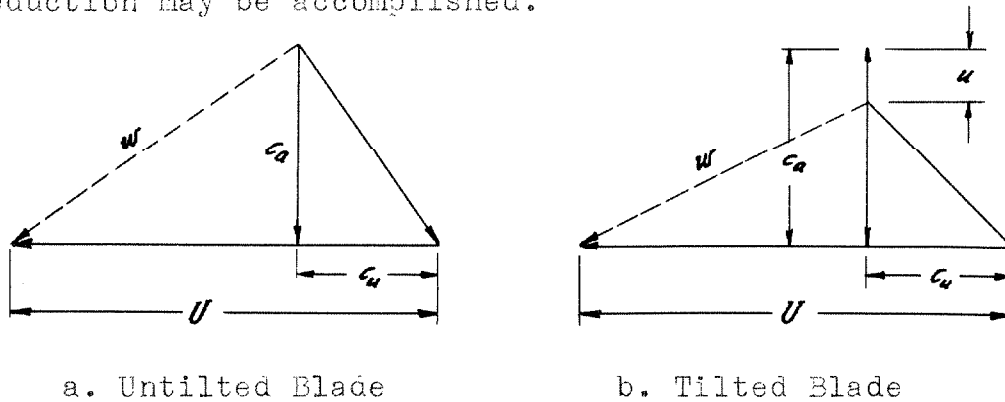


Fig. 10

The following notation is used

$c_a$  = axial velocity at tip with untitled blades

$c_u$  = tangential or whirl velocity at tip

$U$  = velocity of rotor tip

$u$  = axial velocity induced by tilted blades

$w$  = relative velocity at rotor tip

Therefore for no tilting the relative velocity is given by

$$w = \sqrt{c_a^2 + (U - c_u)^2} \quad (52)$$

For tilted blades the relative velocity is

$$w = \sqrt{(c_a - u)^2 + (U - c_u)^2} \quad (53)$$

Now in order to find the relative velocity the axial velocity distribution downstream of the blades must be found.

The following notation will be used

$c_{a1}$  = axial velocity far upstream of blade row

$c_{a2}$  = axial velocity far downstream of blade row

The approximation is also made that the trailing vorticity distribution is a function of  $y$  only, i.e.

$$\left. \begin{aligned} \gamma(\xi, \eta) = \gamma(\eta) &= \frac{\partial c_{a1}}{\partial \eta} & x < 0 \\ &= \frac{\partial c_{a2}}{\partial \eta} & x > 0 \end{aligned} \right\} \quad (54)$$

The Green's function (equation 17) can now be used and it is found that the axial velocity distribution may be written on the form

$$\left. \begin{aligned} c_a &= \sum_{n=1}^{\infty} B_n e^{-\frac{n\pi x}{b}} \cos \frac{n\pi y}{b} + c_{a2}(y) & x \geq 0 \\ c_a &= -\sum_{n=1}^{\infty} B_n e^{\frac{n\pi x}{b}} \cos \frac{n\pi y}{b} + c_{a1}(y) & x \leq 0 \end{aligned} \right\} \quad (55)$$

At  $x = 0$  subtraction of these equations gives

$$2 \sum_{n=1}^{\infty} B_n \cos \frac{n\pi y}{b} = c_{a2} - c_{a1} \quad (56)$$

and from the orthogonality properties of the trigonometric functions this gives

$$B_n = \frac{1}{b} \int_0^b (c_{a2} - c_{a1}) \cos \frac{n\pi y}{b} dy \quad (57)$$

For most practical cases it is sufficient to assume that the change in axial velocity is antisymmetric and linear, i.e.

$$c_{a2} - c_{a1} = \frac{c'}{b} (y - \frac{1}{2}b) \quad (58)$$

This gives for equation (55)

$$\left. \begin{aligned} c_a &= c_{a2} - \frac{2c'}{\pi^2} \sum_{n=0}^{\infty} \frac{\cos \frac{(2n+1)\pi y}{b}}{(2n+1)^2} e^{-\frac{(2n+1)\pi x}{b}} & x \geq 0 \\ c_a &= c_{a1} + \frac{2c'}{\pi^2} \sum_{n=0}^{\infty} \frac{\cos \frac{(2n+1)\pi y}{b}}{(2n+1)^2} e^{-\frac{(2n+1)\pi x}{b}} & x \leq 0 \end{aligned} \right\} \quad (59)$$

Since exponentials die out rapidly it is fairly good to take  $e^{-\frac{(2n+1)\pi |x|}{b}}$  as the governing rate of decrease of the induced velocities, so equation (59) may be written approximately

$$\left. \begin{aligned} c_a &\approx c_{a2} - \frac{1}{2} (c_{a2} - c_{a1}) e^{-\frac{\pi x}{b}} & x \geq 0 \\ c_a &\approx c_{a1} + \frac{1}{2} (c_{a2} - c_{a1}) e^{-\frac{\pi x}{b}} & x \leq 0 \end{aligned} \right\} \quad (60)$$

Equation (60) holds approximately for the case where all

the vorticity change takes place at  $x = 0$ . If the vorticity change takes place at  $x = \xi$ , equation (60) becomes

$$\left. \begin{aligned} c_a &\approx c_{a2} - \frac{1}{2}(c_{a2} - c_{a1})e^{-\frac{\pi(x-\xi)}{b}} & x > \xi \\ c_a &\approx c_{a1} + \frac{1}{2}(c_{a2} - c_{a1})e^{\frac{\pi(x-\xi)}{b}} & x < \xi \end{aligned} \right\} \quad (61)$$

It is now assumed that the vorticity change responsible for  $(c_{a2} - c_{a1})$  is distributed along axial projection of the chord as shown in Figure 11. The object is to find the distribution of the axial velocity.

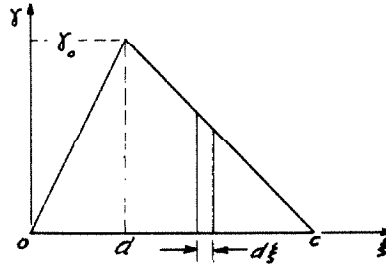


Fig. 11

Assuming that equation (58) holds, this gives

$$\frac{\partial c_{a2}}{\partial y} - \frac{\partial c_{a1}}{\partial y} = \frac{1}{2} \gamma_0 c = \frac{c'}{b} \quad (62)$$

or

$$\gamma_0 = \frac{2c'}{cb} \quad (63)$$

With coordinate system chosen as shown in the figure this also gives

$$\left. \begin{aligned} \frac{d}{dy} \left( d(c_{a2} - c_{a1}) \right) &= \frac{2c'}{cb} \cdot \frac{\xi}{d} d\xi & 0 \leq \xi \leq d \\ \frac{d}{dy} \left( d(c_{a2} - c_{a1}) \right) &= \frac{2c'}{cb} \cdot \frac{(c-\xi)}{(c-d)} d\xi & d \leq \xi \leq c \end{aligned} \right\} \quad (64)$$

Integration of this gives

$$\left. \begin{aligned} d(c_{a2} - c_{a1}) &= \frac{2c'y}{cb} \frac{\xi}{d} d\xi & 0 \leq \xi \leq d \\ d(c_{a2} - c_{a1}) &= \frac{2c'y}{cb} \frac{(c-\xi)}{(c-d)} d\xi & d \leq \xi \leq c \end{aligned} \right\} \quad (65)$$

Then the axial velocity is given by

$$\left. \begin{aligned} c_a &= c_{a1} + \frac{1}{2} \int_0^c d(c_{a2} - c_{a1}) e^{\frac{\pi}{b}(x-\xi)} & x < 0 \\ c_a &= c_{a2} - \frac{1}{2} \int_0^c d(c_{a2} - c_{a1}) e^{-\frac{\pi}{b}(x-\xi)} & x > c \end{aligned} \right\} \quad (66)$$

Carrying through the integration gives

$$\left. \begin{aligned} c_a &= c_{a1} + c' \frac{by}{cd\pi^2} \left( 1 + \frac{ce^{-\frac{\pi d}{b}} + de^{-\frac{\pi c}{b}}}{c-d} \right) e^{\frac{\pi x}{b}} & x < 0 \\ c_a &= c_{a2} - c' \frac{by}{cd\pi^2} \left( 1 + \frac{de^{\frac{\pi c}{b}} - ce^{\frac{\pi d}{b}}}{c-d} \right) e^{-\frac{\pi x}{b}} & x > c \end{aligned} \right\} \quad (67)$$

These are now applied to the two types of blades discussed previously. For the free vortex blades  $c_{a2} = c_{a1}$ , and therefore  $c' = 0$ . For solid body blades it is seen from

Figure 22 that

$$c' = c_{a_2} - c_{a_1} \approx -0.076 \frac{U}{b} \left( \gamma - \frac{b}{2} \right) \quad (68)$$

It is assumed that the leading edge of the rotor is at  $x = 1.2c$ . Giving the constants  $c$  and  $d$  in equation (67) it is then possible to compute the axial velocity entering the rotor at the tip and therefore the relative velocity. Table II below gives these for various combinations of  $c$  and  $d$  with untilted blades.

Table II.

Axial and relative velocities at rotor tip for free vortex and solid body prerotation vanes.

$\frac{c}{b}$	$\frac{d}{b}$	Free Vortex	Solid Body	$\frac{c_a}{U}$	$\frac{w}{U}$
		$\frac{c_a}{U}$	$\frac{w}{U}$		
0.25	0.0625	0.45	0.966	0.384	0.776
0.25	0.1875	0.45	0.966	0.386	0.778
0.125	0.03125	0.45	0.966	0.391	0.780
0.125	0.09375	0.45	0.966	0.392	0.781

For the same values of  $c$  and  $d$  as in Table II the effect of tilting the blades was now computed. The induced axial velocity at the tip is proportional to the tangent of the tilting angle,  $\tan \epsilon = l$  (see Fig. 9). The proportionality factor at  $x = 1.2c$  is shown in Table III below. The pro-



portionality factor multiplied by the tangent of the tilting angle gives the induced axial velocity at the tip in per cent of the approaching axial velocity.

Table III

Proportionality factor giving axial velocity for tilted blades.

$\frac{c}{b}$	$\frac{d}{b}$	Free Vortex	Solid Body
0.25	0.0625	14.75	23.03
0.25	0.1875	17.18	27.26
0.125	0.03125	21.01	34.31
0.125	0.09375	22.94	37.91

The relative velocities may now easily be calculated for any given tilting angle. Table IV shows the axial velocity and relative velocity at the rotor tip due to tilting of 45 degrees. The table also shows the per cent reduction in relative velocity from the relative velocity which is encountered with radial blades.

Table IV

Axial and relative velocities on rotor tip for pre-rotation vanes tilted 45 degrees.

$\frac{c}{b}$	$\frac{d}{b}$	Free Vortex		Solid Body		Per cent reduction in $w$	
		$\frac{c_a}{U}$	$\frac{w}{U}$	$\frac{c_a}{U}$	$\frac{w}{U}$	Free Vortex	Solid Body
0.25	0.0625	0.384	0.937	0.280	0.732	3.00	5.68
0.25	0.1875	0.373	0.931	0.263	0.724	3.62	6.94
0.125	0.03125	0.355	0.925	0.237	0.715	4.25	8.33
0.125	0.09375	0.347	0.922	0.221	0.710	4.56	9.10

For purposes of comparison the following table is reproduced here from Reference 5 (Table I)

Table V.

Relative velocity on rotor for various blade types. All values are given for hub ratio of 0.6 and for 50% reaction point at midradius.

Radial Position $\frac{y}{b}$	Blade Type				
	$\frac{\alpha}{f^2}$	$\frac{\alpha}{f}$	$\alpha$	$\alpha f$	$\alpha f^2$
0	0.40	0.51	0.61	0.65	0.72
0.5	0.70	0.70	0.70	0.71	0.72
1.0	0.96	0.91	0.84	0.76	0.69

For the blade shapes on which calculations have been made throughout this paper, the free vortex blades had their 50% reaction point at  $f = 0.7$  ( $\frac{y}{b} = 0.25$ ), whereas the solid body blades had the 50% reaction point at midradius. However, this difference has only a slight effect on the relative velocities and tables IV and V can be easily compared. It is seen that the reduction in relative velocity ranges from 4.5 per cent for free vortex blades to 9 per cent for solid body blading for the highest aspect ratio blades considered. This reduction in relative velocity, although not large, is very significant for high speed compressors. The relative velocity for the solid body blading approaches the relative velocity for blades of the type  $\frac{C_u}{U} = \alpha f^2$  which was found to be the best

blade type with respect to relative velocity of the five blade types investigated in Reference 5. Such a blade, however, has other disadvantages.

It is therefore concluded from these examples that it will be of definite advantage to lean the blades at an angle to the radial line in a plane perpendicular to the axis of rotation. For maximum reduction in relative velocity the peak loading on the blade should be as close to the trailing edge as possible and the high aspect ratio blades have a definite advantage over low aspect ratio blades.

# REFERENCES

1. Prandtl, L. and Tietjens, O. G.: "Applied Hydro- and Aeromechanics", McGraw-Hill, 1934.
2. Marble, F. E. and Michelson, I.: "Analytical Investigation of Some Three-dimensional Flow Problems in Turbomachines", NACA T.N. 2614, March, 1952.
3. Meyer, Richard E.: "Beitrag zur Theorie feststehender Schaufelgitter", Mit. Inst. Aerodynamik E.T.H., Zurich, 1946.
4. Marble, F. E.: "The Flow of a Perfect Fluid through an Axial Turbomachine with Prescribed Blade Loading", Journal of the Aeronautical Sciences, Vol. 15, No. 8, August, 1948.
5. Rannie, W. Duncan, et al.: "Theoretical and Experimental Investigations of Axial Flow Compressors", Summary Report, Contract N6-ori-102, Task Order IV, Office of Naval Research, Mechanical Engineering Laboratory, C.I.T., January, 1949.

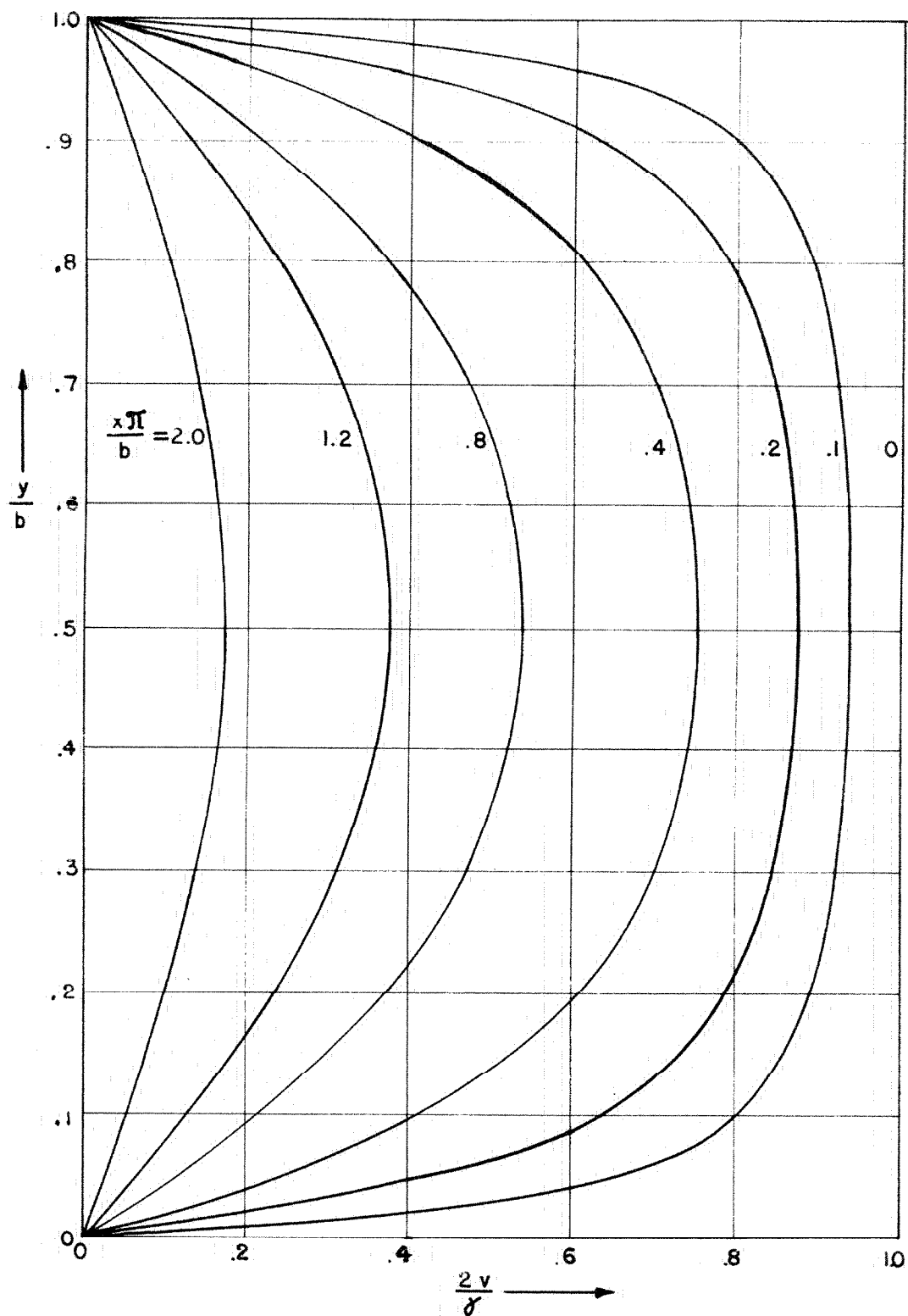
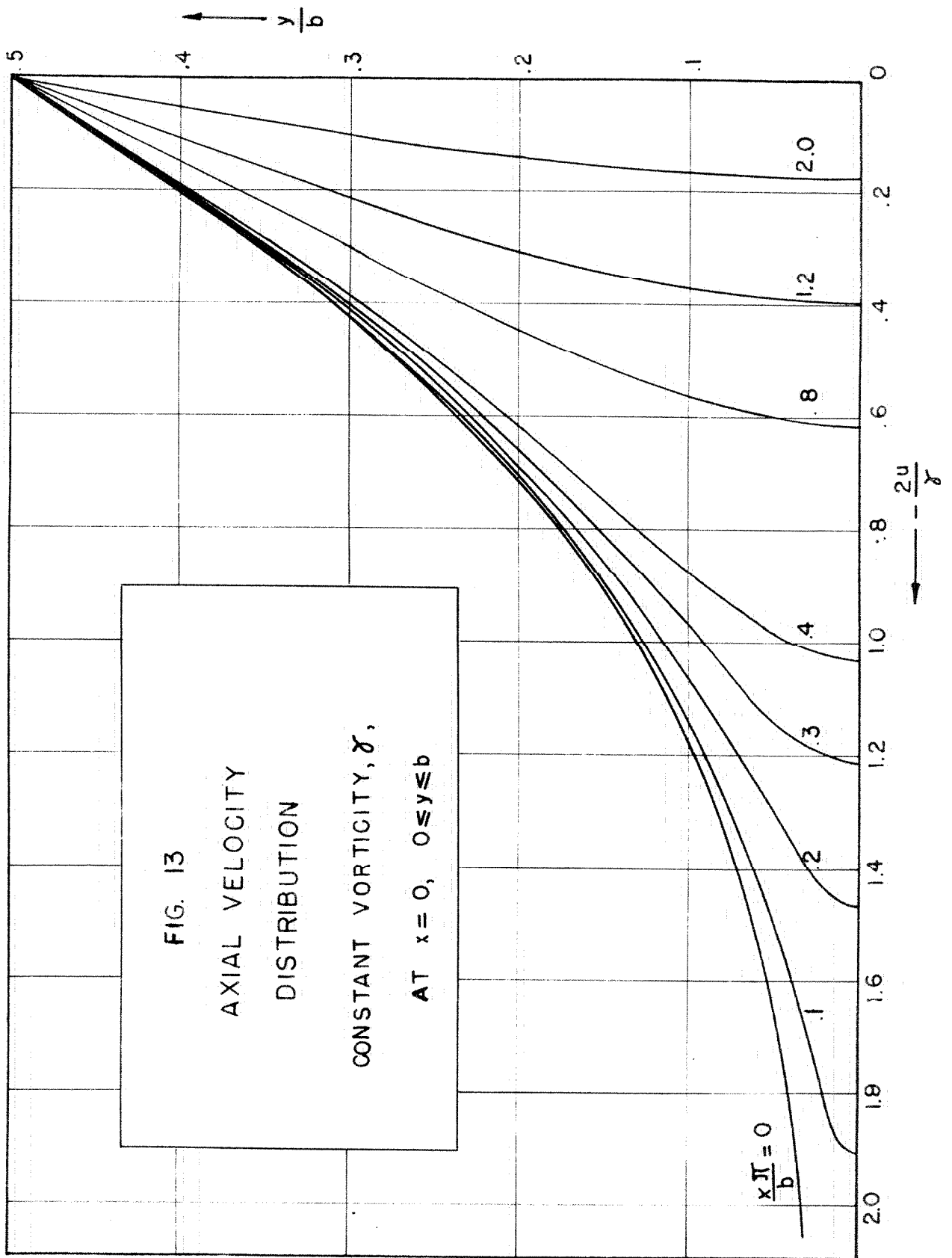
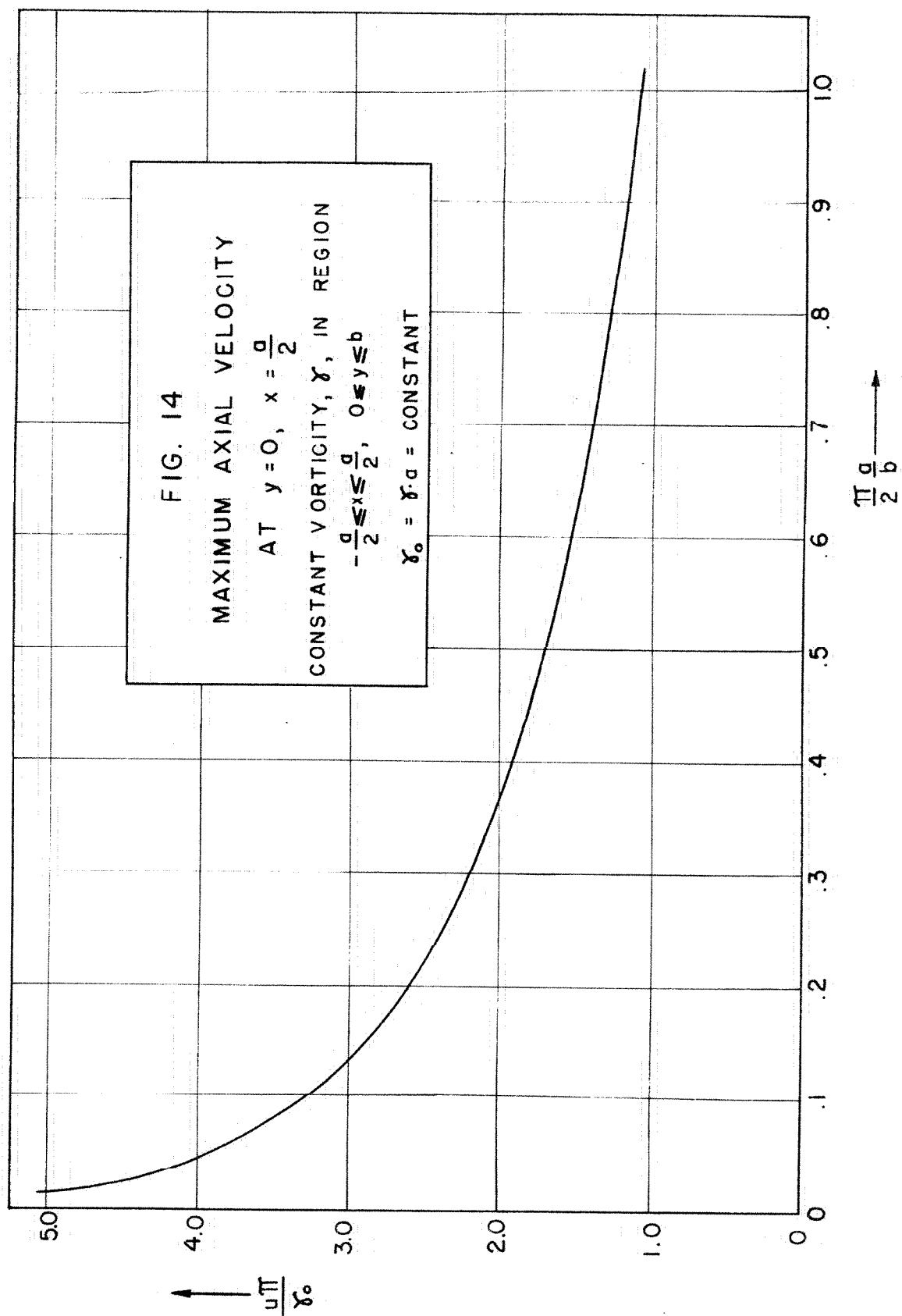
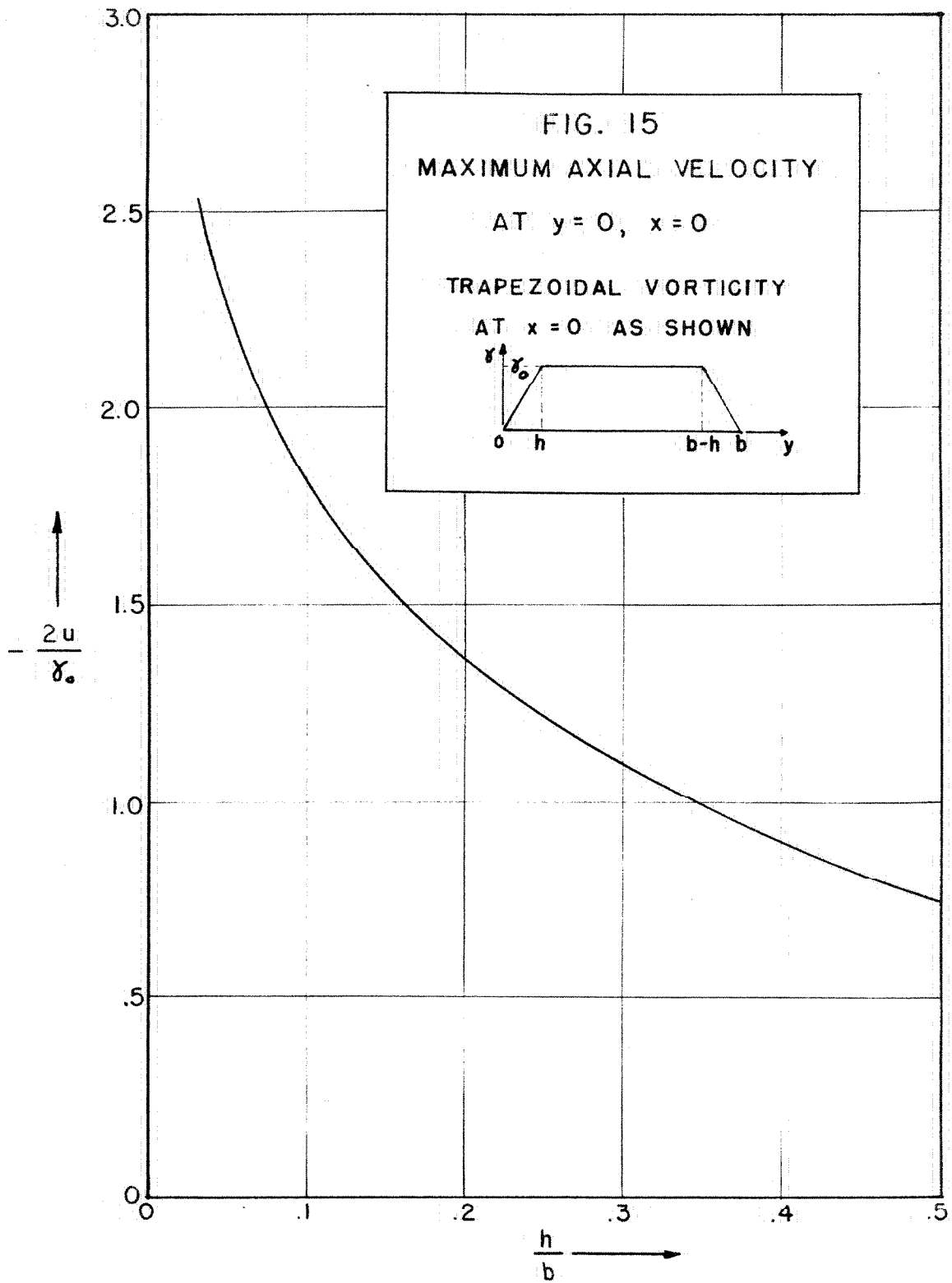


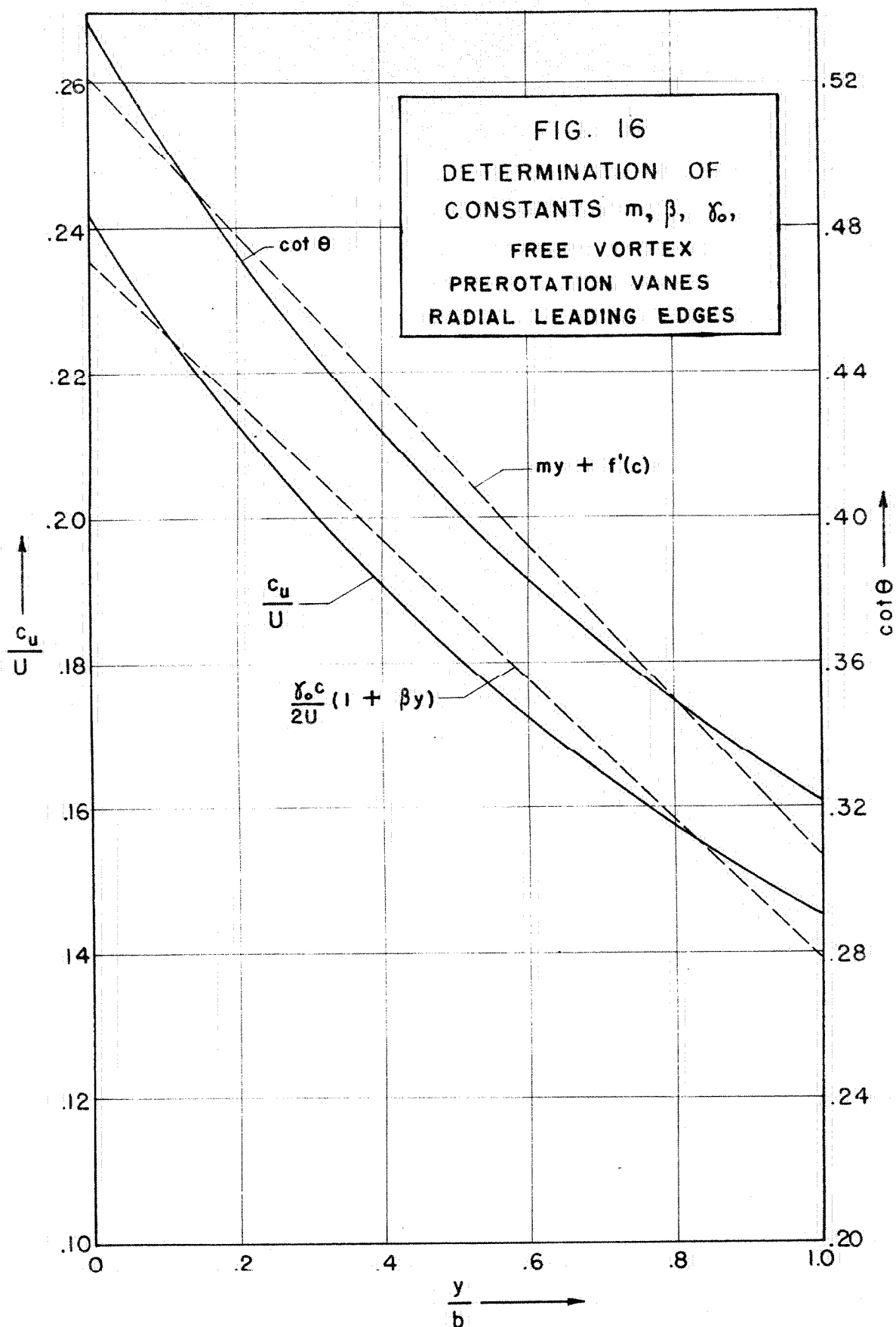
FIG. 12  
 RADIAL VELOCITY DISTRIBUTION  
 CONSTANT VORTICITY,  $\gamma$ , AT  $x=0$ ,  $0 \leq y \leq b$

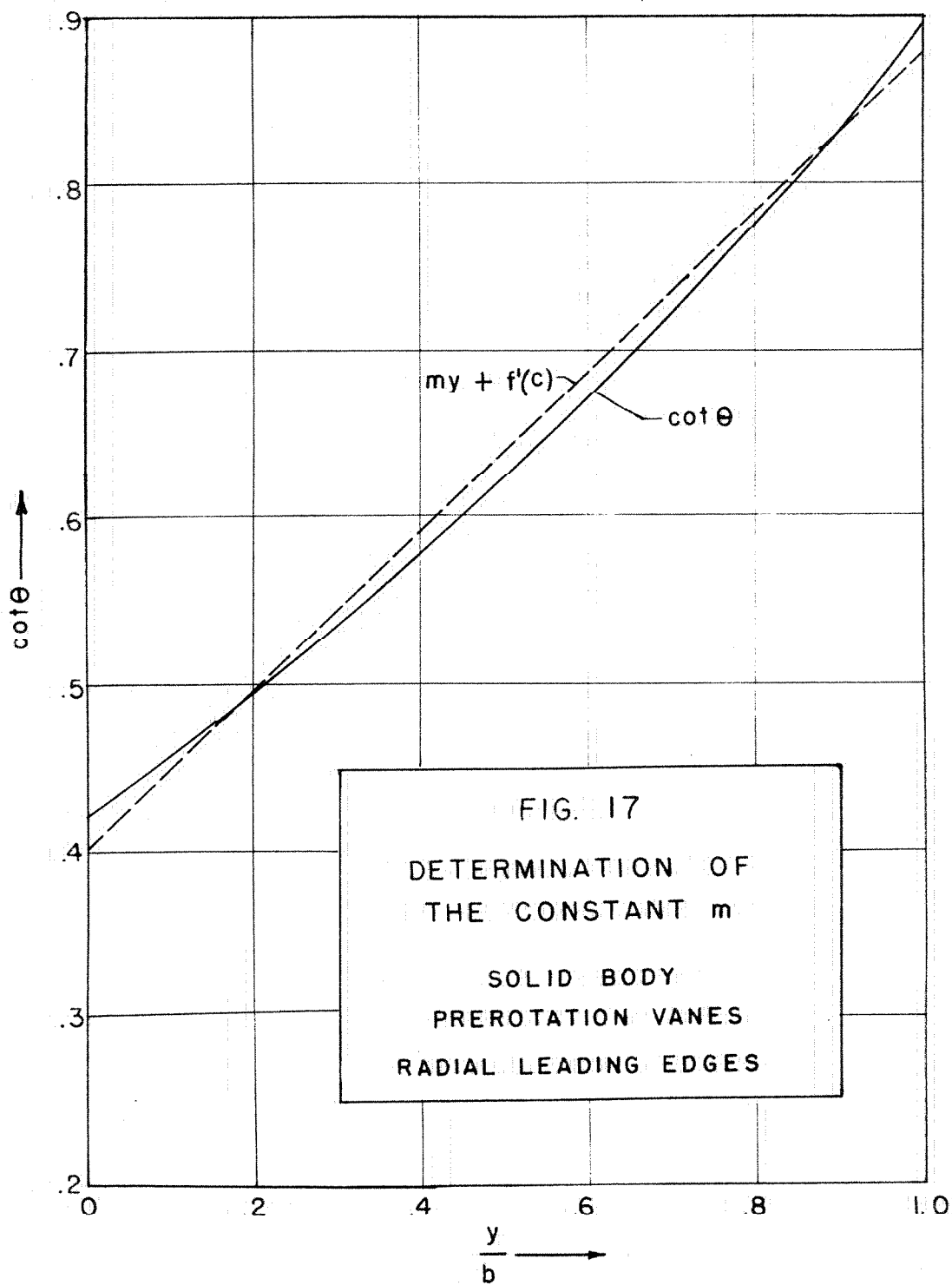












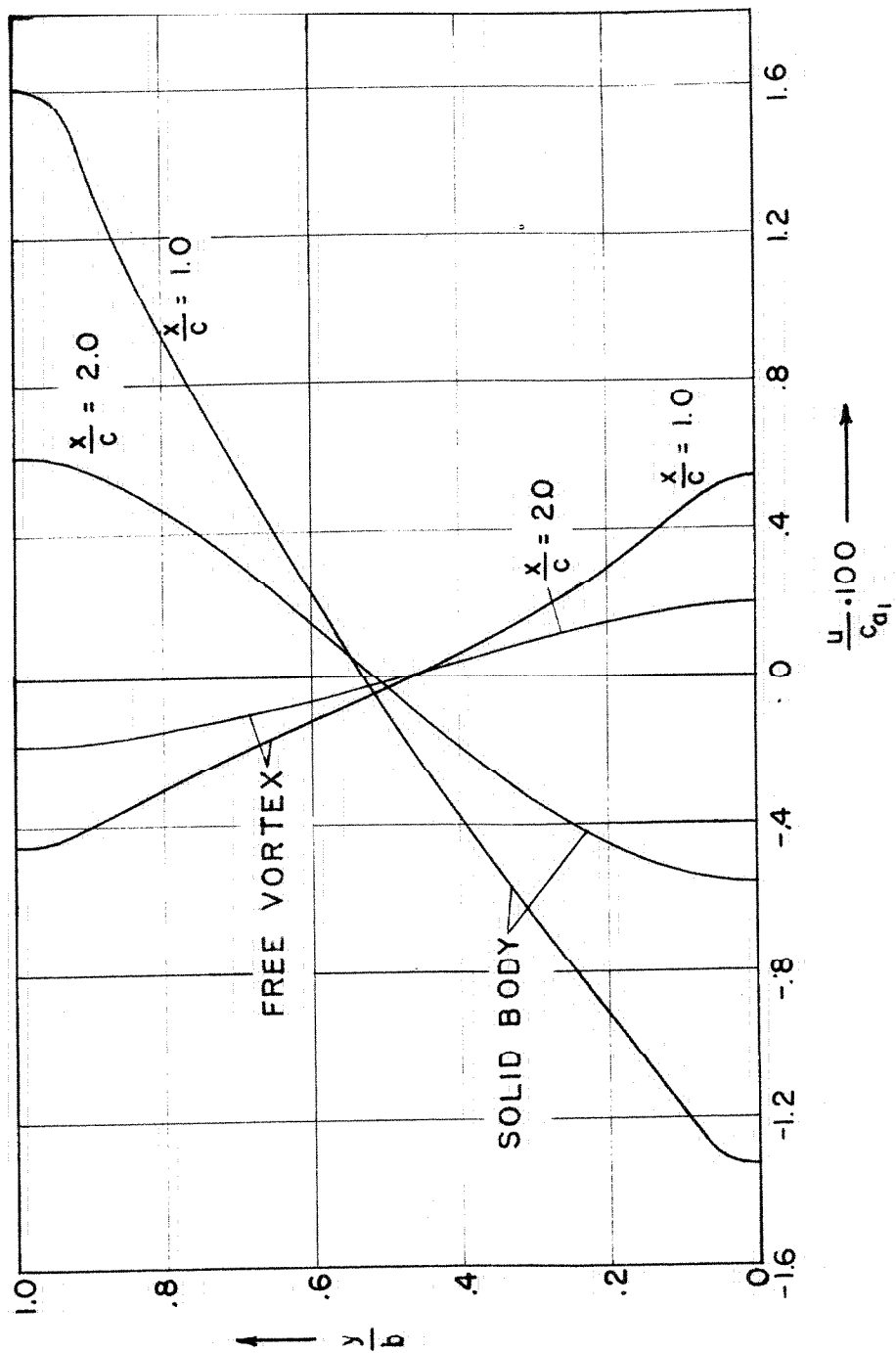


FIG. 18  
 AXIAL VELOCITY DISTRIBUTION BEHIND BLADES  
 PREROTATION VANES — RADIAL LEADING EDGES

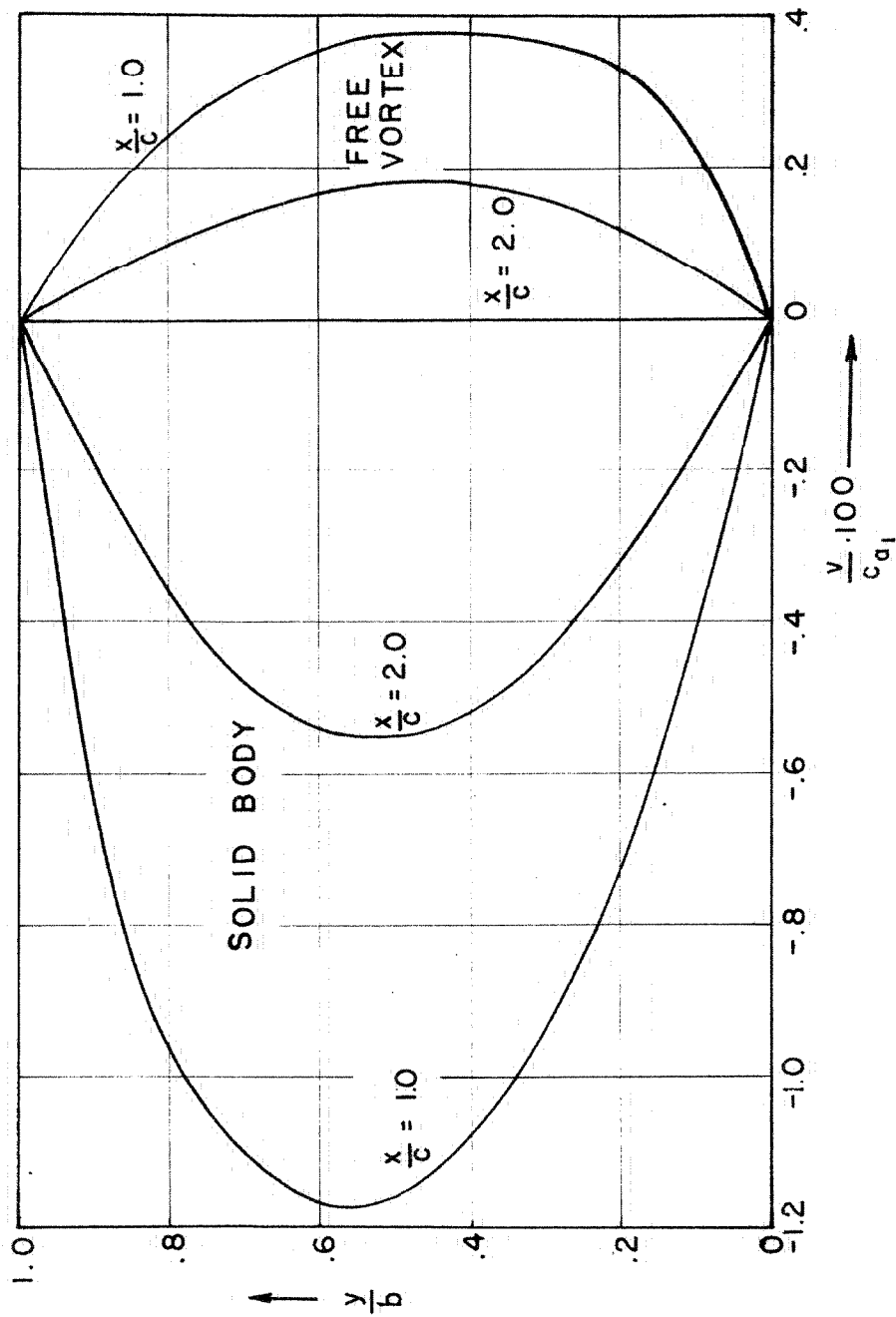


FIG. 19  
 RADIAL VELOCITY DISTRIBUTION BEHIND BLADES  
 PREROTATION VANES — RADIAL LEADING EDGES

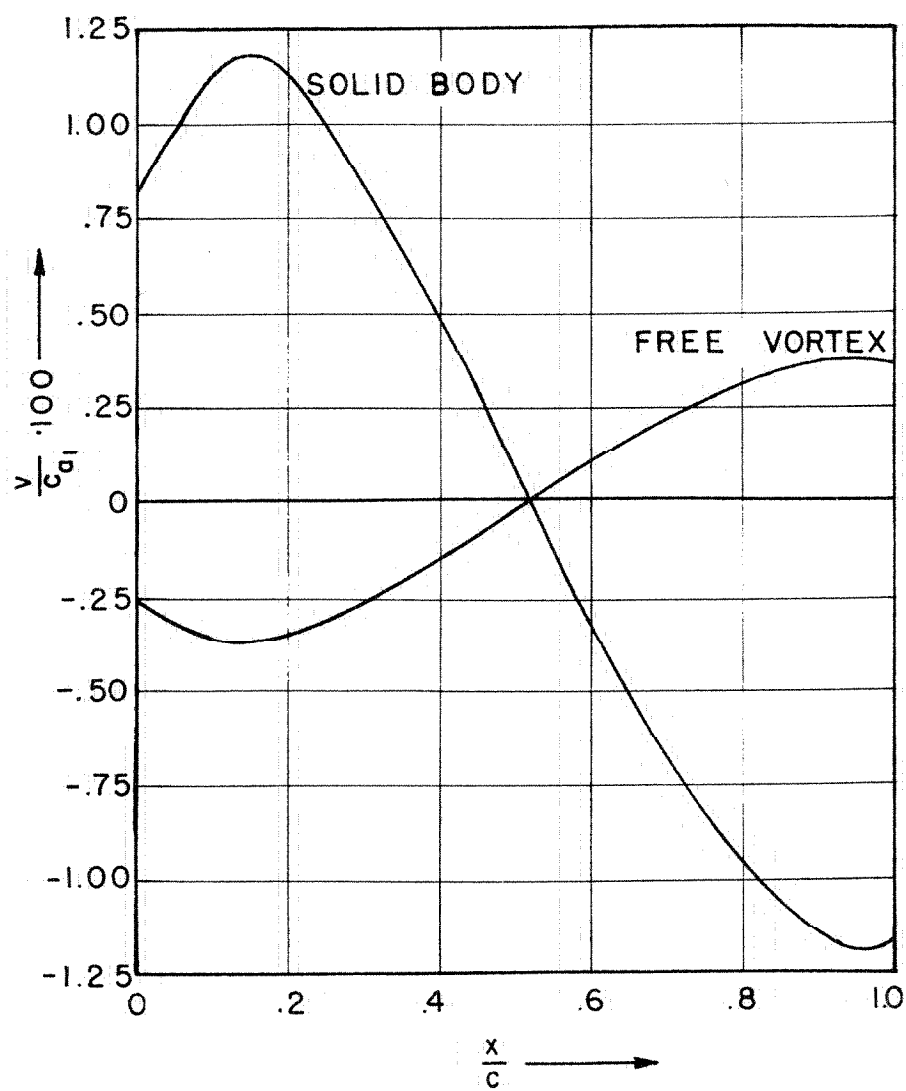


FIG. 20

RADIAL VELOCITY DISTRIBUTION  
THROUGH VANES AT MIDRADIUS

PREROTATION VANES  
RADIAL LEADING EDGES

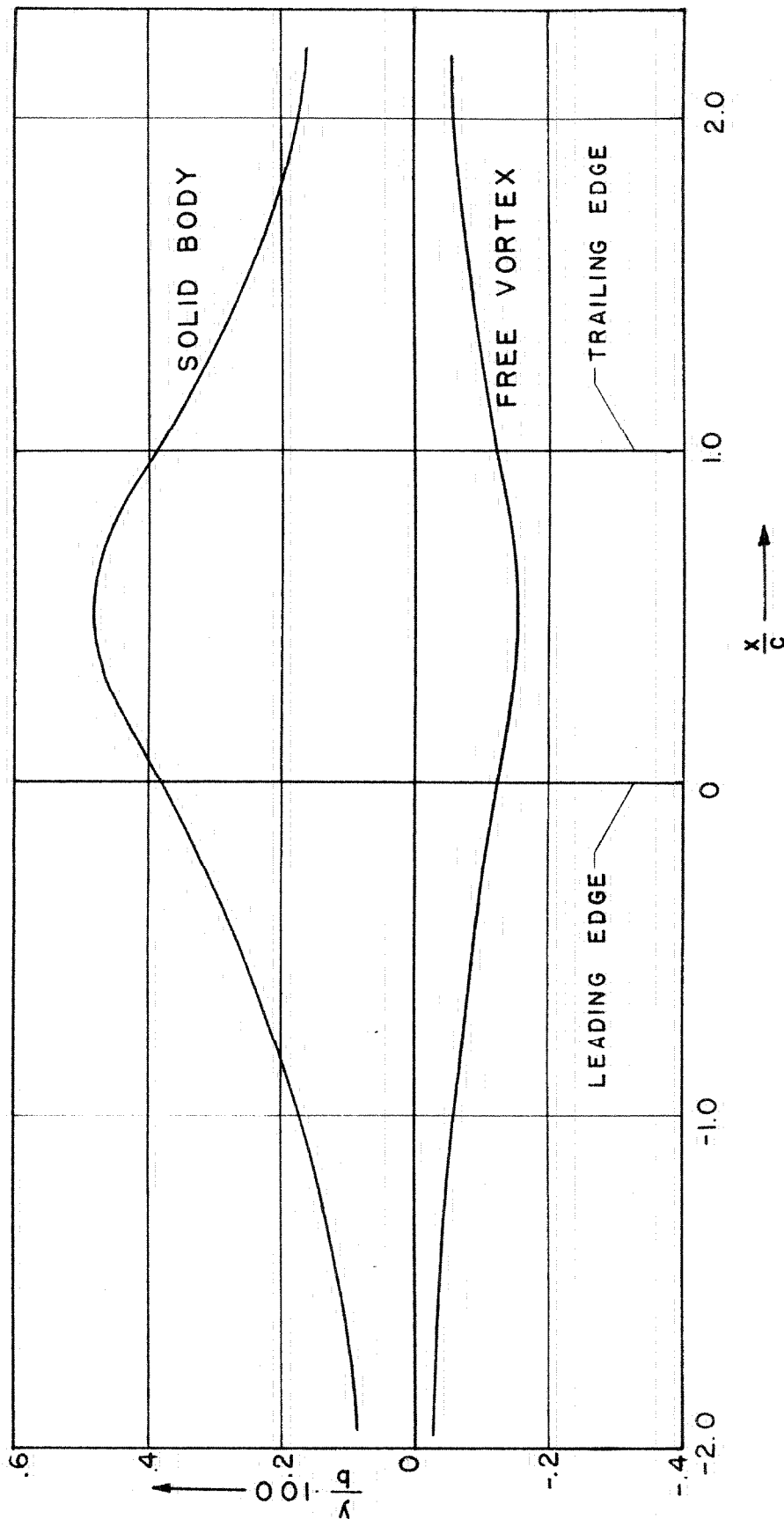


FIG. 21

DEFLECTION OF STREAMLINES THROUGH BLADE ROW AT MIDRADIUS

PREROTATION VANES — RADIAL LEADING EDGES

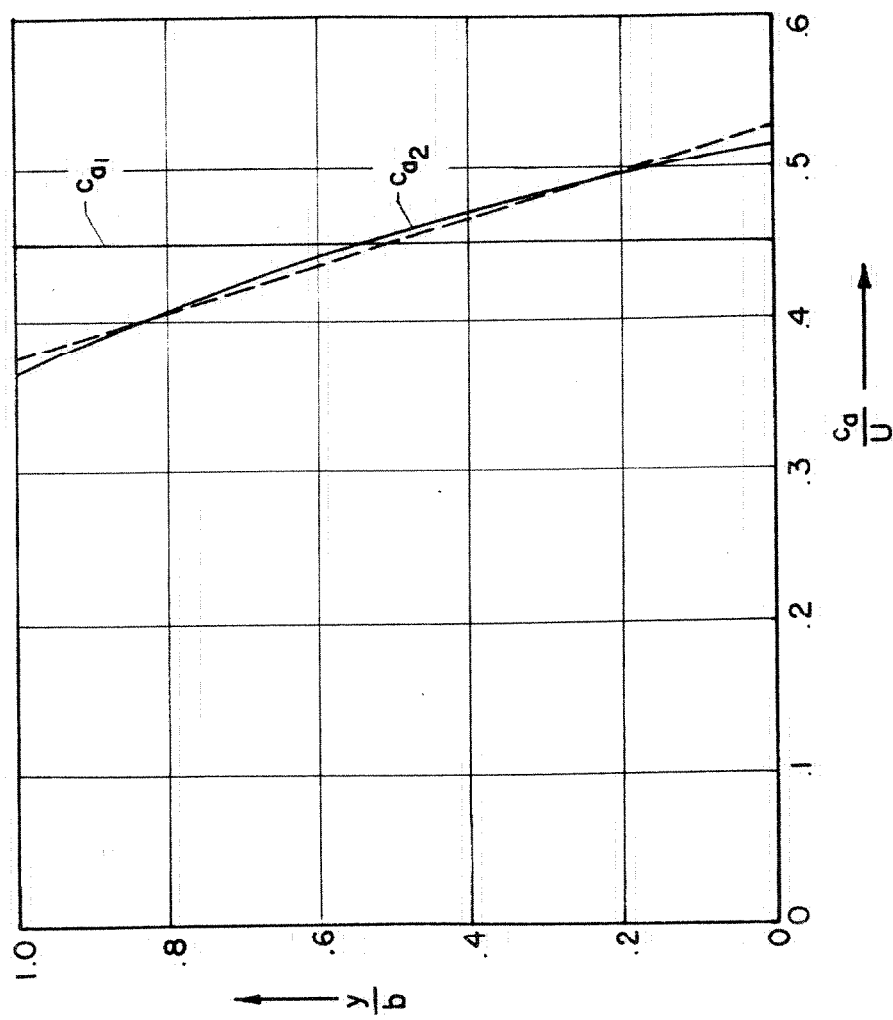


FIG. 22  
DISTRIBUTION OF MAIN AXIAL VELOCITY  
SOLID BODY BLADING